

# Loss Calculation for High Speed Permanent Magnet Claw Pole Outer Rotor Machine

**Guangwei Liu, Xingang Zhao, Zhao Xin, Fengge Zhang**

*School of Electrical Engineering, Shenyang University of Technology, 110870, China*

*Corresponding author's e-mail: DRGuangwei\_Liu@yeah.net*

*Received 1 March 2013, www.cmnt.lv*

## Abstract

In view of higher frequency electromagnetic field and higher speed rotation comparing with conventional machine, the loss of high speed claw pole permanent magnet outer rotor machine should be considered seriously. In this paper, its structure and operation principle was introduced, and the three dimension magnetic field distribution is analyzed. A new iron loss calculation model is built in consideration of three-dimension quadrature alternative and harmonic magnetic field. In addition, the calculation model of air friction loss and its influencing factors, such as rotor speed, surface roughness and axial ventilation speed, are analyzed. The results of the finite element analysis validate accuracy of that of theory analysis.

*Keyword:* high speed motor, permanent magnet rotor, claw pole machine, loss calculation

## 1 Introduction

In recently years, the increasing attention has been given to high speed drives for wider range of industrial applications, such as flywheel energy storage, compact micro generation gas turbines, aircraft electrical starter-generator systems and compressors [1-2]. Among these applications, the key device is a high speed rotating electrical machines in the direct drive application. The direct drives system remove mechanical transmission coinciding with weight reduction, the system efficiency increase and the failure reduction can be obtained [3-4].

In order to achieving the higher volumetric power density and efficiency improvement, one of permanent magnet (PM) motor design trends is on the direction of an more and more higher rotational speed. But most high speed PM motors with inner rotor structure, for which the carbon-fiber bandage must be used to against centrifugal force and to fasten the magnets on the rotor surface. So the equivalent air-gap length is increase and efficiency of heat dissipation is decreased. Hence, another structure of outer rotor high speed synchronous motor is proposed, the PMs mounted on inner surface of high speed rotor is endured pressure stress caused by centrifugal force, so the bandage can be removed [5-6].

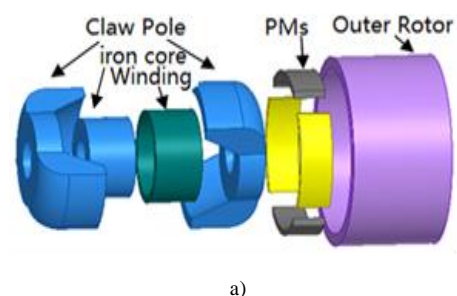
The soft magnetic composite (SMC) is an isotropic material in terms of magnetic and mechanical properties, which makes the design of magnetic circuits in electrical machines in three dimensions. Compared with laminated steel for electric machine, the SMC material typically in material performance tests has lower saturation induction, however with lower core loss at high frequency [7-8].

So a high speed claw pole outer PM rotor machine (CPMOPMR) with SMC is proposed. It has many advantages such as high efficiency, high power density, without PM bandage, but because of complicated structure and

high speed rotation, the loss calculation of CPMOPMR is different from traditional PM machine. In this paper, three dimension quadrature alternation magnetization calculation model to approximate rotation magnetization was built to calculate loss accurately by three methods. For a high-speed machine the air friction loss on PM surface lead to permanent magnet demagnetization, and its influencing factors, such as rotor speed, surface roughness and axial ventilation speed were analyzed in this paper through the three-dimensional flow field software.

## 2 Structure and operation principle

The CPMOPMR consists of several claw pole stators and PM outer rotor. Stator is composed by several claw pole sections with same arrangement in axial direction, which are machined by SMC, and in circumferential direction angle difference of each section is equal, which is relative to the number of section. Several PMs are mounted at inner surface of outer rotor, which is made by 45# steel, and their arrangement is corresponding to pole number [9]. Each phase concentrated winding is mounted on the shaft of one section claw pole. The structure of CPMOPMR for 4 poles single-section is shown in Fig.1. The parameters of CPMOPMR are shown in table 1



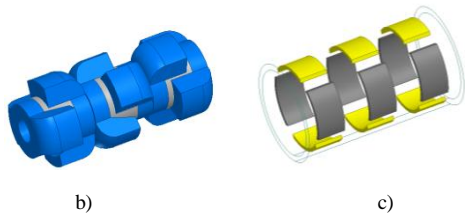


FIGURE 1 Diagram of structure for CPMOPMR:  
a) Single section; b) Claw pole stator; c) PM outer rotor

Table 1 Motor parameters

parameters	value	parameters	value
Rated Power /W	6000	Core length /mm	550
Rated voltage /V	270	Gap length /mm	1
Rated speed /(r/min)	40000	Permanent magnet length /mm	27
Rated frequency /Hz	1333	Permanent magnet width /mm	47
Poles/number	4	Permanent magnet thickness /mm	3
Turns/number	27	Claw length /mm	20
One section Motor length /mm	53	Claw tip width/mm	33
Stator Diameter /mm	75	Claw root width/mm	33
Stator core diameter/mm	40.4	Circular iron core length /mm	25
Winding diameter/mm	47	Outer rotor thickness/mm	6
Shaft diameter /mm	20	Parallel branches	3

### 3 Main loss in claw pole motor

#### 3.1 IRON LOSS

Due to the higher frequency than conventional machine, the iron loss of CPMOPMR is more serious. Traditionally, there is only iron core loss caused by the alternating magnetic field in motor. In fact, the rotating core loss caused by rotational magnetization need to be concerned also when the motor running. In order to completely understand the magnetization process, it is necessary to build rotating magnetic iron loss calculation model based on the research of radial, tangential and axial magnetization characteristics of CPMOPMR. To avoid the disadvantage that rotating loss testing equipment cannot get easily, three dimensional orthogonal alternating iron loss calculation model can be built to replace rotational magnetic model [10]. The three dimensional flux density of CPMOPMR can be expressed by:

$$\vec{B}(t) = \vec{B}_r(t) + \vec{B}_\theta(t) + \vec{B}_z(t), \quad (1)$$

where  $\vec{B}_r(t)$ ,  $\vec{B}_\theta(t)$  and  $\vec{B}_z(t)$  are the radial, tangential and axial components of rotating magnetic field separately [11].

Then the iron losses of any position can be calculated by sum of each direction, which can be expressed by:

$$P_{Fe} = K_h f (B_{rm}^\alpha + B_{\theta m}^\alpha + B_{zm}^\alpha) + K_e f^2 (B_{rm}^2 + B_{\theta m}^2 + B_{zm}^2) + \frac{K_e}{(2\pi)^{3/2}} \left( \frac{1}{T} \int_0^T \left( \left| \frac{dB_r(t)}{dt} \right|^2 + \left| \frac{dB_\theta(t)}{dt} \right|^2 + \left| \frac{dB_z(t)}{dt} \right|^2 \right) dt \right) \quad (2)$$

In order to study the magnetization characteristics in various portions of the claw pole stator, the several key points of each portion are selected, and they can be the equivalence of the magnetization characteristics of whole part, For example, the selected key points at the end portion of claw pole are shown in Fig.2. Then, the motor magnetic field is calculated by finite element method, and where the curve of flux density and vector at any point for three directions are obtain, the results at point a are shown in Fig. 3 and 4.

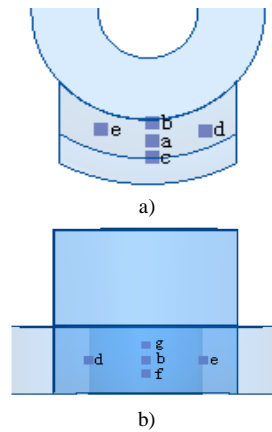


FIGURE 2 Key points of the end of claw pole:  
a) Claw pole motor front view; b) Claw pole motor plan view

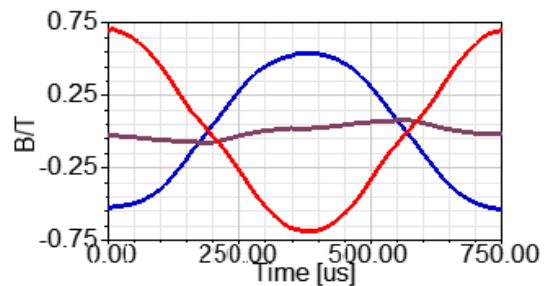


FIGURE 3. Flux density of point "A"

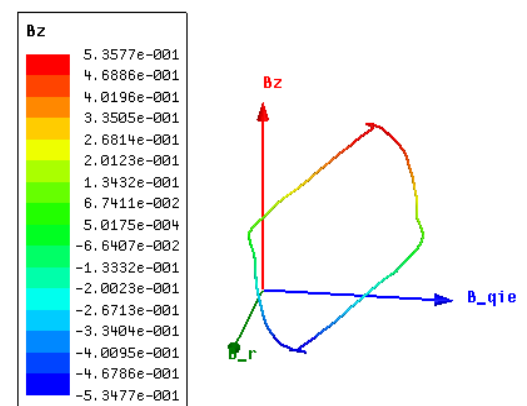


FIGURE 4 Vector flux density of point "A"

From analyzing and comparing the results of flux density at 7 points of the end portion of claw pole, the average flux density amplitude value at point b and c is equal to that of point a, at the same time, which of point f and g is equal to that of point a. So the flux density at point a can be used to be the equivalence of that at radial section of end section where point a located. In addition, the flux density at point d is equal to that of point e because their locations are near to claw pole root. Due to the flux density in different parts of claw pole are not equal, the claw pole are divided into several portions to calculate iron loss. The curves of flux density at various portions of claw pole stator are shown in Fig 5.

Because the variation range of flux density amplitude at claw knee part is very small, the average value of several points at claw knee can be used to replace that at the whole knee. At the same time, the claw is divided into three parts, which includes claw root part, claw middle part and claw tip part. Due to little change of flux density amplitude at each part, so the average flux density amplitude of one point or several points are used to replace claw each part respectively to calculate iron loss. So the iron loss can be derived as follows

$$P_{Fe} = \sum_{i=1}^n (P_{ei} + P_k + P_{cs} + P_{cm} + P_{ce} + P_s), \quad (3)$$

where  $P_{cs} = 1.2671P_{ce}$ ,  $P_{ce} = 0.4397P_{cm}$  ;

$P_{ei}$  is claw end iron loss;  $P_k$  is claw knee iron loss;

$P_{cs}$  is claw root part iron loss;  $P_{cm}$  is claw middle part iron loss;  $P_{ce}$  is claw tip part iron loss;  $P_s$  is circle core part iron loss;

The iron loss calculated by simplified calculation model is reduced obviously. In order to verify the feasibility of iron loss calculation method, Flux density amplitude of each subdivision unit is taken out and put into (2) to get iron loss. The result is compared to the simplified model.

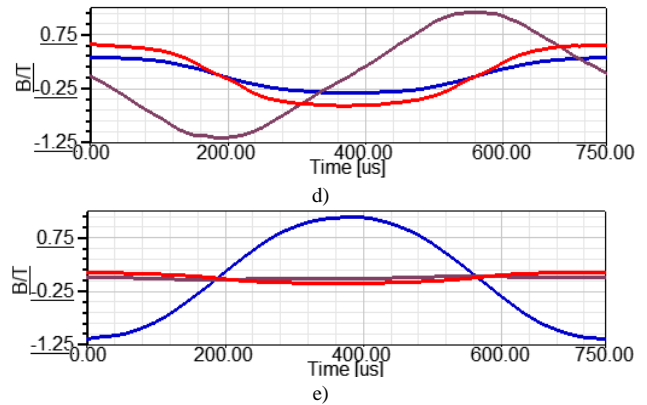
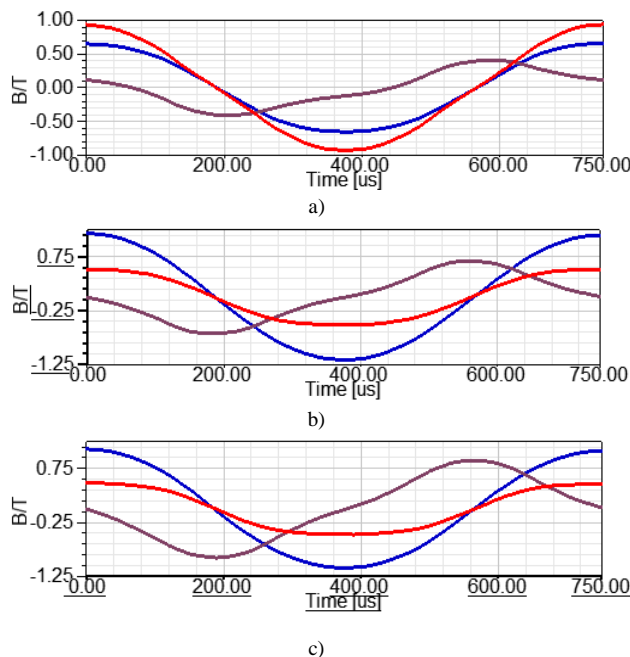


FIGURE 5 Flux density of claw pole:

- a) Flux density of claw knee part; b) Flux density of claw root part;
- c) Flux density of claw middle part; d) Flux density of claw tip part;
- e) Flux density of circle core part

As shown in Fig 6, iron loss value calculated by the exact calculation method and simplified calculation method are almost same. Due to the rotation magnetization have not been considered in finite element software, the results by the finite element calculation are lower than other two. Three dimensional orthogonal iron loss calculation models are verified correctly, which reduce the optimization design workload for this kind of motor.

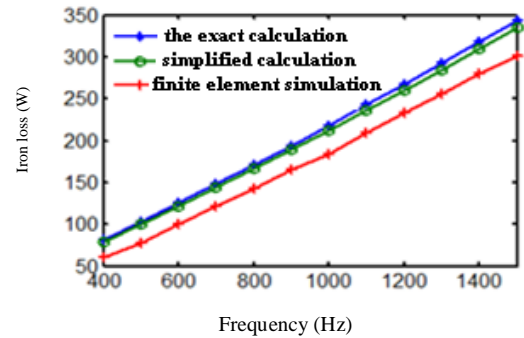


FIGURE 6 Iron loss of three methods

### 3.2 THE AIR FRICTION LOSS

For a high-speed machine, the rotor surface air friction loss is much greater than that of a low speed one. The permanent magnets may be demagnetization, and even the motor damaged, caused by this loss. So it is necessary to analyze and calculated the air friction loss of PM rotor surface. The air friction loss of the cylindrical rotor surface can be derived as follows;

$$P_{af} = kC_f \pi \rho_{air} \omega_m^3 r^4 l \quad (4)$$

$$C_f = \frac{0.0152}{Re^{0.24}} \left[ 1 + \left( \frac{8}{7} \right)^2 \left( \frac{4Re_a}{Re_\delta} \right)^2 \right]^{0.38} \quad (5)$$

$$\text{for: } Re_\delta = \frac{\rho_{air} \omega_m r \delta}{\mu_{air}} \quad Re_a = \frac{\rho_{air} v_a 2\delta}{\mu_{air}}$$

Where  $k$  is the roughness of the rotor surface;  $C_f$  is the coefficient of friction;  $l, r$  is the length and radius of outer rotor;  $\omega_m$  is rotational angular velocity;  $\delta$  is the length of gap;  $\mu_{air}$  is the moving air viscosity;  $v_a$  is the axial wind speed of force air cooling.

In order to prevent the permanent magnets demagnetizing caused by B. The air friction loss, the epoxy resin as a filler could be added to gaps of PMs to make the rotor surface smooth. By this method the roughness of the rotor surface can be effectively reduced, so as the air friction loss decrease.

The air friction loss of a high-speed machine includes not only the friction of fluid and wall, but also the different form between the import and export of fluid channel. Therefore, the analytical formulas applying to the turbulent fluid could not get accurate results. In this paper, the fluid field finite element software is used to analyze the air friction loss of the claw pole high speed motor with permanent magnet outer rotor. The effect of rotor surface roughness, rotation speed and the length of gap on the air friction loss could be accurately analyzed.

The boundary conditions can be given as follows:

- 1) The fluid import was speed import, export is pressure import. The pressure at the export is atmospheric pressure.
- 2) The inner surface of rotor is the boundary for the motion. The speed and roughness at rotor inner surface were designated.
- 3) Other boundary is insulation boundary.

Heat release coefficient of water is the given value, and the interface of cooling air and the motor are arranged as fluid-solid coupling interface. Due to the characteristics of the structure, the flow of cooling air and heat transfer in motor is very complex. To solve the problems, some boundary conditions are given:

- 1) Air duct inlet is given for mass flow, which is as entrance boundary condition. Air volume of entrance and temperature are set.
- 2) Air duct outlet is set as pressure outlet boundary condition, and the outlet pressure is standard atmospheric pressure.
- 3) All symmetry planes on both sides of notch are rotating periodic boundary condition.
- 4) Contact surface of air duct and rotor is set for moving wall, whose rotation speed is 1885rad/s, to simulate rotation of the rotor.

So the calculation method of the total energy change can be derived as follows:

$$Q = h_f(T_w - T_f) + q_{rad}, \tag{6}$$

where,  $h_f$  is the heat conduction coefficient of fluid,  $T_w$  is the temperature of the wall,  $T_f$  is the temperature of the fluid,  $q_{rad}$  is heat radiation flux.

Based on the fluid field model, the temperature distribution of motor can be calculated only considering air friction loss, which is shown in Fig.7, the temperature rise from import to export is no more than 18°.

The air friction loss under different speed is calculated, and the results are shown in Fig.8. According to comparing both, we know that the rotation speed has a great influence on the air friction loss, and it could be expressed by

$$P_{air} = kn^\alpha, \tag{7}$$

where  $n$  is speed;  $k, \alpha$  is undetermined coefficient;

By fitting to the curve by the least square method from Fig.6, the fact that  $\alpha$  is equal to 2.591 could be obtained. The air friction of motor is not only related to speed, but also related to roughness, axial wind speed and other factors. The relationships between the air friction loss and roughness, axial wind speed are respectively shown in Fig.9 and 10.

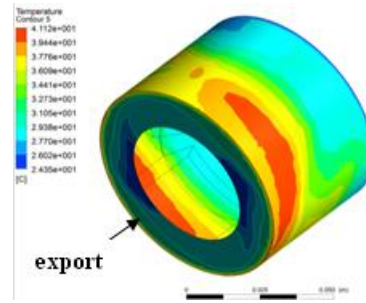


FIGURE 7 The temperature distribution

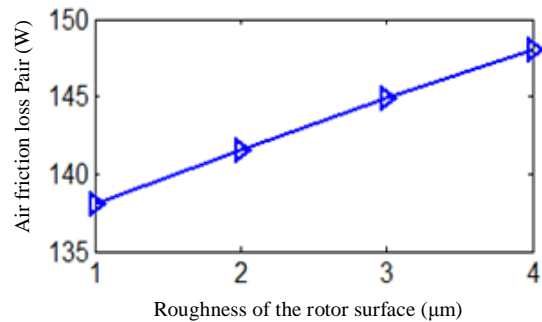


FIGURE 8 The air friction vs. roughness

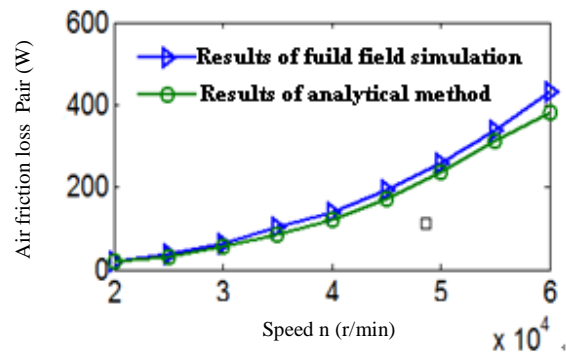


FIGURE 9 The air friction vs. speed

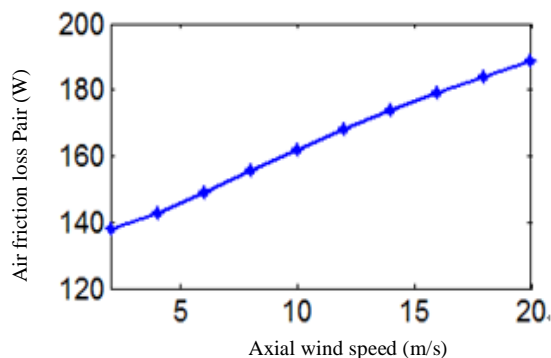


FIGURE 10 The air friction vs. axial wind speed

From the above analysis, the fact that the greatest effect factor on the air friction is rotation speed can be known, which has the exponential growth trend. In addition, to increase the axial speed has some effect to take heat away, but increasing speed will increase the air friction loss. Therefore, not only the roughness of rotor surface should be reduced, also the appropriate cooling wind speed should be selected.

From above analysis, all loss of prototype can be obtained, which is shown in Tab. 2

Table 2 Loss of CPMOPMR

projects	Iron loss	Copper loss	Air friction loss	Eddy current loss of PM
loss/W	876	54	138	73

## References

- [1] Zlatko Kolondzovski, Antero Arkkio, Jaakko Larjola 2011 Power Limits of High-Speed Permanent-Magnet Electrical Machines for Compressor Applications *IEEE Trans. on Energy Conversion* **1** 26
- [2] Zhu Z Q, Ishak D, Howe D, Chen J 2013 Influence of slot and pole number combinations on unbalanced magnetic force in PM machines with diametrically asymmetric windings *IEEE Trans. Ind. Appl.* 49
- [3] Jahns T M 2010 The Expanding Role of PM Machines in Direct-Drive Applications *Int. Conf. on Elec. Machines and Systems*, August 20-3 Beijing, China
- [4] Borisavljevic A, Polinder H, Ferreira A 2010 On the speed limits of permanent-magnet machines[J]. *IEEE Transactions on Industrial Electronics* **1** 57
- [5] Guo Y G, Zhu J G, Dorrell D G 2009 Design and analysis of a claw pole permanent magnet motor with molded soft magnetic composite core *IEEE Trans. Magn.* 45
- [6] Jurca F N, Martis C 2012 Theoretical and experimental analysis of a three-phase permanent magnet claw-pole synchronous generator *IET Electric Power Applications* **8** 6
- [7] Guo Y G, Zhu J G, Lu H 2012 Core loss calculation for soft magnetic composite electrical machines *IEEE Transactions on Magnetics* **11** 48
- [8] Xing Junqing, Wang Fengxiang 2010 Research on Rotor Air Friction Loss of High-speed Permanent Magnet Machines *Proceedings of the CSEE* **27** 30
- [9] Zhang Fengge, Liu Guangwei 2012 Magnetic Circuit Model and Parameter Calculation of a Claw Pole Machine with Outer PM Rotor *Transactions of China Electrotechnical Society* **6** 27
- [10] Tang Renyuan 1997 Modern Permanent Magnet Machines *Theory and Design*. China Machine Press
- [11] Huynh C, Zheng Liping, Acharya D 2009 Losses in high speed permanent magnet machines used in micro turbine applications *Journal of Engineering for Gas Turbines and Power* 131

## 4 Conclusion

In this paper, a new calculation model is built to calculate iron loss accurately by ways of three-dimension orthogonal alternation magnetization as equivalent substitution of rotation magnetization. The stator core loss of CPMOPMR is calculated accurately by combined with finite element simulation. And the effect factors on the air friction loss were researched, such as motor speed, the rotor surface roughness and axial wind speed.

## Acknowledgment

This work is supported by program for Changjiang Scholars and Innovative Research Team in University (IRT1072), project supported by National Natural Science Foundation of China (51077094, 51207094).

## Authors



**Guangwei Liu, born on 14 May 1983, Zhengzhou China**

**Current position, grades:** Lecture

**University studies:** Shenyang University of Technology

**Scientific interest:** special motor design and its control system

**Publications:** 19

**Experience:** He received his B.S. and M.S. degree in Electrical Engineering from Shenyang University of Technology, China in 2005 and 2008 respectively. Now he is a lecture in Shenyang University of Technology, and study as a Ph.D. student in the School of Electrical Engineering



**Xingang Zhao, born on 2 May 1989, Shenyang China**

**Current position, grades:** Master student

**University studies:** Shenyang University of Technology

**Scientific interest:** high speed permanent magnet machine

**Publications:** 1

**Experience:** He received the B.S degree in University of Science and Technology Liaoning. He is currently working toward the M.S degree in the School of Electrical Engineering, Shenyang University of Technology, Liaoning, China. Since 2013, he has been with the Shenyang University of Technology



**Zhao Xin, born on 23 Nov 1983, Shenyang China**

**Current position, grades:** Engineer

**University studies:** Shenyang University of Technology

**Scientific interest:** permanent magnet machine

**Publications:** 3

**Experience:** She received her B.S. degree of Automation from Shenyang Institute of Aeronautical Engineering in 2005, and M.S. degree of Control Theory and Control Engineering from China in 2008. Now she is an engineer in Shenyang University of Technology



**Fengge Zhang, born on 18 Mar 1963, Yutian China**

**Current position, grades:** Professor

**University studies:** Shenyang University of Technology

**Scientific interest:** special motor design and its control system

**Publications:** 107

**Experience:** He received his B.S., M.S. and Ph.D. in Electrical Engineering from Shenyang University of Technology, Shenyang, China in 1984, 1990 and 2000, respectively. He is director of the Department of Electrical Machines Engineering in the School of Electrical Engineering at Shenyang University of Technology.